Hum Genet (2008) 123:41–53
DOI 10.1007/s00439-007-0447-7

ORIGINAL INVESTIGATION

A novel KCNQ4 pore-region mutation (p.G296S) causes deafness by impairing cell-surface channel expression

Ángeles Mencía · Daniel González-Nieto · Silvia Modamio-Høybjør · Ainhoa Etxeberría · Gracia Aránguez · Nieves Salvador · Ignacio del Castillo · Álvaro Villarroel · Felipe Moreno · Luis Barrio · Miguel Ángel Moreno-Pelayo

Received: 30 June 2007 / Accepted: 9 November 2007 / Published online: 21 November 2007

Abstract Mutations in the potassium channel gene *KCNQ4* underlie DFNA2, a subtype of autosomal dominant progressive, high-frequency hearing loss. Based on a phenotype-guided mutational screening we have identified a novel mutation c.886G>A, leading to the p.G296S substitution in the pore region of KCNQ4 channel. The possible impact of this mutation on total KCNQ4 protein expression, relative surface expression and channel function was investigated. When the G296S mutant was expressed in *Xenopus* oocytes, electrophysiological recordings did not show voltage-activated K^+ currents. The p.G296S mutation impaired KCNQ4 channel activity in two manners. It greatly reduced surface expression and, secondarily, abolished channel function. The deficient expression at the cell surface membrane was further confirmed in non-permeabilized NIH-3T3 cells transfected with the mutant KCNQ4 tagged with the hemagglutinin epitope in the extracellular S1–S2 linker. Co-expression of mutant and wild type KCNQ4 in oocytes was performed to mimic the heterozygous condition of the p.G296S mutation in the patients. The results showed that the G296S mutant exerts a strong dominant-negative effect on potassium currents by reducing the wild type KCNQ4 channel expression at the cell surface. This is the first study to identify a trafficking-dependent dominant mechanism for the loss of KCNQ4 channel function in DFNA2.

Á. Mencía · S. Modamio-Høybjør · I. del Castillo · F. Moreno · M. Á. Moreno-Pelayo (✉)
Unidad de Genética Molecular, Hospital Ramón y Cajal, Carretera de Colmenar Km 9, 28034 Madrid, Spain
e-mail: mmoreno.hrc@salud.madrid.org

Á. Mencía · S. Modamio-Høybjør · I. del Castillo · F. Moreno · M. Á. Moreno-Pelayo
Centre for Biomedical Research on Rare Diseases (CIBERER), Madrid, Spain

D. González-Nieto · L. Barrio
Departamento de Investigación, Hospital Ramón y Cajal, Unidad de Neurología Experimental, 28034 Madrid, Spain

A. Etxeberría · Á. Villarroel
Unidad de Biofísica, CSIC-UPV/EHU, 48940 Bilbao, Spain

G. Aránguez
Servicio de ORL, Hospital General Universitario Gregorio Marañón, 28007 Madrid, Spain

N. Salvador
Instituto Cajal, CSIC, 28002 Madrid, Spain

Introduction

Hearing impairment is a very common sensory defect in humans. Non-syndromic hereditary forms, in which the hearing loss is the only clinical sign, have been proven to be genetically very heterogeneous. So far, more than 90 genetic loci for non-syndromic hereditary hearing loss have been mapped, and for more than 40 of them the responsible genes have been identified (Petersen 2002, 2006; Friedman et al. 2003). One of these genes, *KCNQ4* (MIM#603537), maps to 1p34, within the DFNA2 genetic interval, and encodes the voltage-gated potassium $K_v7.4$ channel protein. Typically these channels comprise four subunits that encircle a central pore, which enables the selective passage of potassium ions across the cell membrane. Each subunit consists of six transmembrane segments (S1–S6), with both N-and C-termini on the intracellular side of the membrane. The S4 segment contains the voltage-sensor of the channel; and the S5 and S6 segments, along with an intervening re-entrant loop (P-loop domain), form the pore region. Four

P-loops combine to form the selectivity filter of the channel (Doyle et al. 1998). All missense mutations and deletions identified so far in *KCNQ4* have been associated with DFNA2, a subtype of autosomal dominant non-syndromic sensorineural progressive hearing loss (ADNSHL) in which the high frequencies are initially affected. This phenotype is consistent with the predominant pattern of KCNQ4 expression and native K^+ currents primarily mediated by homomeric KCNQ4 channels in the sensory outer hair cells (OHCs) of basal turns of the cochlea (Kubisch et al. 1999; Kharkovets et al. 2000, 2006). Missense mutations are generally associated with earlier onset and more severe hearing impairment than deletions, suggesting that the phenotypic differences may be caused by distinct mechanisms of pathogenesis. The two deletions identified so far truncate the protein before the first transmembrane domain (Coucke et al. 1999; Kamada et al. 2006), and hence they can cause haploinsufficiency with an expected reduction of 50% in channel activity. In contrast, the missense mutations have been reported to exert a dominant-negative effect on wild type function causing a higher reduction in channel activity (Kubisch et al. 1999; Jentsch 2000). Interestingly, most of the missense mutations occur within the P-loop domain in the pore region of KCNQ4 channel (Kubisch et al. 1999; Coucke et al. 1999; Talebizadeh et al. 1999; Van Hauwe et al. 2000; Akita et al. 2001; Van Camp et al. 2002; Topsakal et al. 2005). The mechanism underlying the effect of dominant-inhibition has not been identified yet.

In this study, we report on the identification of a novel missense mutation (p.G296S) in the pore region of the KCNQ4 channel that segregates with postlingual and progressive ADNSHL in a Spanish family. Expression and functional studies carried out in *Xenopus* oocytes and transfected NIH-3T3 cells reveal that the G296S mutant exerts a strong dominant-negative effect on wild type channel activity by causing a defect in trafficking of KCNQ4 channels to the cell surface membrane.

Patients and methods

The protocols of this study were approved by the Institutional Review Board of Hospital Ramón y Cajal (Madrid, Spain).

Clinical data of family S300

A four-generation family, S300, was ascertained through the Hospital General Universitario Gregorio Marañón, Madrid, Spain (Fig. 1a). After getting written informed consent from all participants, peripheral blood samples were collected from all members of generation III and IV and DNA extraction was performed following standard methods. Clinical history ruled out environmental factors as the cause of the hearing loss in the family and physical examination did not reveal any evidence of syndromic features. Tympanometry indicated proper functioning of the middle ear. Pure-tone audiometry was performed to test for air conduction (125–8,000 Hz) and bone conduction (250–4,000 Hz). Affected subjects show postlingual, bilateral, symmetrical and progressive sensorineural hearing impairment at mid and high frequencies. The earliest clinical evidence of hearing loss in the family was obtained from individual IV:5 at the age of 5 years (Fig. 1b). Initially mild, the hearing loss becomes moderate very quickly. Affected subjects of the family did not exhibit either tinnitus or clinical features suggestive of vestibular dysfunction. Tests for transient-evoked otoacoustic emissions (TEOAEs) and auditory brainstem responses (ABRs) were performed in the two patients of the last generation, IV:5 and IV:1, at the age of 9 and 17 years, respectively. TEOAEs were evaluated in terms of whole reproducibility measures. This method performed better that TEOAE amplitude levels in the prediction of auditory thresholds (Balatsouras et al. 2004). Reproducibility scores higher than 70% correspond to normal TEOAEs. As standard procedure, whole reproducibility was calculated as the mean of the partial scores obtained in the frequency bands of 0.5–1, 1–2, 2–3, 3–4 and 4–5 kHz. Both patients, IV:1 and IV:5, showed abnormal whole reproducibility measures, indicating that the activity of the cochlear OHCs is affected. In patient IV:1, the TEOAEs were completely absent in the left ear and present in the right ear but exhibiting an abnormal whole reproducibility score of 35%. Similarly, patient IV:5 (the youngest affected subject in the family) had bilaterally abnormal whole-reproducibility scores of 44 and 39% for the right and left ears, respectively. The acoustic threshold, when evaluated in the frequency range of 1–2 kHz with the ABR test, was of 55 dB for both ears in subject IV:5 and of 50 and 60 dB for the right and left ear, respectively, in subject IV:1. For higher sound levels ABRs were present bilaterally exhibiting no distortion or alteration of the wave latency and interlatency measurements.

Molecular genetic methods

The microsatellite markers D1S2730, D1S255 and D1S2722 from the DFNA2 region were used to genotype the family S300 (Coucke et al. 1994; Van Camp et al. 1997). Primers and PCR conditions were taken from the Généthon human linkage map (Dib et al. 1996) and from the Marshfield chromosome 1 map (http://research.

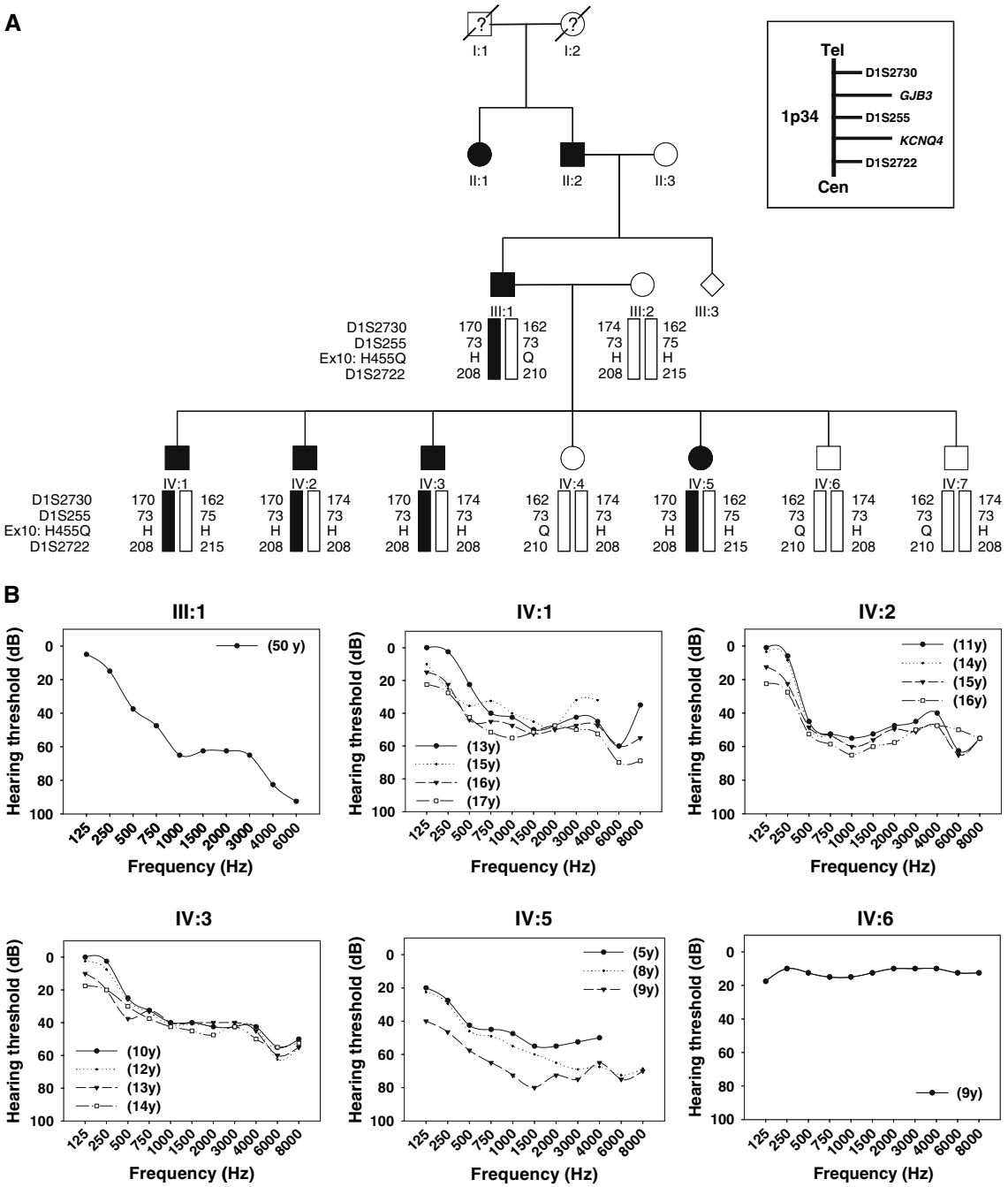

Fig. 1 **a** Pedigree of the Spanish family S300. Affected members are shown in *black*. Genotyping and haplotype analysis for microsatelite markers on chromosome 1 revealed the critical DFNA2-region, identified in the Spanish family with hearing impairment. *Black bars* indicate the affected and white bars the unaffected chromosomes, respectively. The *numbers* placed beside chromosomes are the allelic sizes for each microsatellite marker. The *box* shows the relative order of the *GJB3* and *KCNQ4* genes and the microsatellite markers used for genotyping and haplotype analysis of the DFNA2 genetic interval. The polymorphic position Histidine(H)/Glutamine(Q) located at *KCNQ4* exon 10 is notated as Ex10:H455Q. **b** Audiograms showing the air conduction values obtained from the five different affected patients (III:1, IV:1, IV:2, IV:3, IV:5), and an unaffected family member (IV:6). The age of the patients to which each audiometric record was obtained is indicated. Each graph point represents the average hearing loss for the right and left ears

marshfieldclinic.org/genetics) and the fluorescently labelled alleles were analyzed in an ABI PRISM 3100 automated DNA genetic analyzer (Applied Biosystems, Foster City, CA, USA). Primers were designed to PCR-amplify exons and adjacent intron/exon boundaries of the *KCNQ4* gene (MIM#603537, GenBank accession number NM_004700). Exons 5 and 6 amplimers generated from affected subjects of the different families enrolled in this

study were evaluated for the presence of heteroduplex in MDE gels (BioWhittaker, Rockland, ME, USA). Sequences of PCR products were analyzed in the ABI PRISM 3100 (Applied Biosystems).

Members of family S300 and control subjects were screened for the novel mutation c.886G>A by digesting exon 6 amplimers with *DdeI* restriction enzyme and running the digestion products in agarose gels. Wild type amplimers yield three fragments of 194, 45 and 18 bp. When the mutation is present, the 194 bp fragment is cleaved in two of 116 and 78 bp.

In addition, primers were designed to amplify all exons of the *GJB3* gene (MIM#600101) encoding connexin 31 to exclude the presence of pathogenic mutations in the S300 family.

Expression in *Xenopus laevis* oocytes and voltage-clamp studies

The KCNQ4 wild type ($KCNQ4_{WT}$) full-length cDNA cloned into a pTLN vector (Lorenz et al. 1996) was mutagenized using the Quick Change Site-Directed Mutagenesis Kit (Stratagene) to generate $KCNQ4_{G296S}$ and $KCNQ4_{H455Q}$ variants and subsequently verified by sequencing. After linearization of KCNQ4 constructs with *HpaI*, capped cRNA was synthesized in vitro using the SP6 mMessage mMachine kit (Ambion). *Xenopus* oocytes were defolliculated enzymatically with 1 mg/ml collagenase in calcium free OR2 solution (82.5 mM NaCl, 2.5 mM KCl, 1 mM $MgCl_2$, and 5 mM HEPES, pH 7.5) and then transferred to ND96 calcium-containing solution consisting of (in mM) 96 NaCl, 2 KCl, 1.8 $CaCl_2$, 1 $MgCl_2$, and 5 HEPES, pH 7.5. Oocytes were injected with 50 µl of a solution containing 0.5, 5 or 10 ng of wild type or mutant cRNA. In co-expression experiments, 5 ng or 10 ng of a 1:1 mixture of WT+G296S; H455Q+G296S and WT+H455Q KCNQ4 cRNAs were injected per oocyte. Three days after injection, two-electrode voltage-clamp measurements were performed in oocytes at room temperature using a virtual-ground Geneclamp 500B amplifier (Axon Instruments, Foster City, CA). The oocytes were perfused continuously in *Xenopus* saline made with (in mM) 100 NaCl, 2.5 KCl, 1 $MgCl_2$, 2 $MnCl_2$, and 5 HEPES, pH 7.5. Data were acquired at a sampling rate of 1 kHz and filtered at 100 Hz; voltage-step protocols and current analysis were performed with pCLAMP 8.1 software (Axon Instruments). The voltage activation of KCNQ4 channels was determined as previously described (Kubisch et al. 1999): oocytes were clamped for 3 s from a holding potential of −50 mV to voltages between −120 to +50 mV in 10 mV steps, and followed by a constant pulse to −20 mV of 1.8 s duration. The current activated at different voltage test pulses was estimated by measuring the amplitude of corresponding tail currents at -20 mV. For each oocyte, currents I, were normalized relative to its maximal value induced by the +50 mV pulse. To evaluate the voltage dependence of potassium channels, the mean values of currents (±SE) were plotted versus voltage, and the I/V relationship was fitted to a Boltzmann function of the form:

$$I = I_{max}/[1 + \exp((V_{1/2} - V_m)/\text{slope})]$$

where I_{max} is the maximal current and $V_{1/2}$ is the membrane potential (V_m) at which $I = I_{max}/2$.

Fits were made by treating I_{max}, $V_{1/2}$ and slope as free parameters, and the best values of constants were obtained by applying an iterative procedure of fitting to minimize the least-squares error between data and the calculated fit point (SigmaPlot, Jandel Scientific).

Cell surface biotinylation and Western blot analysis

Cell-surface proteins were biotinylated (35 oocytes per reaction) with the membrane-impermeable *N*-hydroxy-succinimide-SS-biotin (NHS-SS-biotin; Pierce). Oocytes injected 72 h before with wild type and mutant KCNQ4 cRNAs, alone and in combination, were incubated in biotinylation reagent (1.5 mg/ml) for 30 min at 4°C in ND96 calcium-containing solution, pH 8.0. After washing five times in ND96 with 100 mM glycine, oocytes were homogenized in lysis buffer (100 mM NaCl, 50 mM Tris–Cl, pH 7.4, 0.5 mM EGTA, 0.5 mM EDTA, 1% Triton X-100, 25 µg/ml leupeptin, and 1 mM phenylmethylsulphonylfluoride) in a volume of 350 µl (10 µl/oocyte) and maintained on ice for 30 min. After centrifugation at 16,000*g* (4°C) for 15 min, a 5 µl aliquot (1/70) of the supernatant was mixed 1:1 with SDS-PAGE sample buffer (50 mM Tris–Cl, pH 6.8, 50 mM DTT, 2% SDS, 10% glycerol, 5% βME), and stored on ice before SDS-PAGE to asses total KCNQ4 (surface plus internal proteins). Then, 50 µl of streptavidin-coated agarose beads (Sigma) were added to the remaining supernatant (69/70), and samples were rolled at 4°C for 3 h to allow the streptavidin to bind biotinylated proteins. The biotin–streptavidin bead complexes were then washed five times with lysis buffer with a 2-min centrifugation (16,000*g*) between washes. The final pellets were dissolved in 30 µl of SDS-PAGE sample buffer and heated at 25°C for 2 h to cleave the disulfide bonds. The proteins were separated in 7.5% SDS-PAGE gels and transferred electrophoretically to nitrocellulose membranes. After blocking with 5% skimmed dry milk in 1% TBS (pH 7.6)/0.1% Tween 20 for 1 h at room temperature, the blots were incubated overnight at 4°C with the primary rabbit anti-KCNQ4 antibody (1:300 dilution; kindly provided by T.J. Jentsch) directed against carboxy-terminal peptides

(Kharkovets et al. 2000). After washing, the first antibody was detected by a secondary sheep anti-rabbit IgG antibody (1:1,000) conjugated with horseradish peroxidase for 1 h at room temperature. Bands were visualized by the enhanced chemiluminiscence (ECL; Amersham Biosciences) and exposed to X-ray film. Band intensities from Western blots were determined by densitometry (ImageQuant TL software V. 2003.02; Amersham Biosciences).

Epitope-tagged constructs

The anti-KCNQ4 antibody used in Western blot analysis is directed against the C terminus of the protein and it cannot be used to detect the channel expression at the cell surface in non-permeabilized cells. Hence, KCNQ4 alleles cloned into pTLN vector were tagged with a modified hemagglutinin (HA) epitope in the extracellular loop that connects transmembrane domains S1 and S2 of the KCNQ4 channel, as previously described for KCNQ2/Q3 channels (Schwake et al. 2000; Etxeberria et al. 2004). To increase the accessibility of the HA epitope, we enlarged this short loop (STIQEHQELANE) by flanking the epitope with fragments from the extracellular D1–D2 loop of the ClC-5 chloride channel. These insertions change the sequence between transmembrane domains S1 and S2 to (aa)STIQEHQELANE*NSEH***YPYDVPDYA***VTFEERDKCPEWN*C(aa) (HA epitope is shown in bold type, and residues derived from ClC-5 in italics). These mutants were constructed by PCR and verified by sequencing. Both the human untagged and the HA-tagged *KCNQ4* cDNA alleles were subcloned into the bicistronic pIRES-hrGFP-1a expression vector (Stratagene) from the corresponding pTLN constructs described above.

Cell culture and transfection

The NIH-3T3 cell line was cultured in DMEM medium supplemented with 10% fetal calf serum (FCS), 100 units/ml of penicillin, and 100 μg/ml of streptomycin over 12 mm coverslips (Menzel-Glaser, GmbH, Braunschweig, Germany) in flat-bottom 24-well multititer plates (Falcon; BD Biosciences, San Jose, CA) for immunochemistry studies. Cells were transiently transfected with 400 ng of HA-KCNQ4$_{WT}$ or mutated HA-KCNQ4$_{G296S}$ tagged constructs using JetPEI (Qbiogene) transfection reagent according to the manufacturer's directions.

Immunocytochemistry

Cells on coverslips were fixed, 68 h after transfection, in 4% paraformaldehyde in phosphate buffer 0.1 M NaH_2PO_4 pH 7.04 for 10 min and then washed three times briefly in PBS. To study intracellular protein localization, cells were permeabilized for 10 min at room temperature with 0.5% Triton X-100 in PBS. Permeabilized and non-permeablized cells were blocked with 3% BSA in PBS for 30 min, washed with PBS twice and incubated for one hour at room temperature with a 1:500 dilution of the rat monoclonal antibody to HA epitope (3F10, Roche) or with the rabbit affinity purified antisera raised against KCNQ4 carboxy-terminal peptides (kindly provided by Dr. Jentsch) (Kharkovets et al. 2000). Cells were washed three times with PBS, and then incubated for 1 h at room temperature with a 1:500 dilution of the secondary antibody; Alexa Fluor™ 594 conjugated goat anti-rabbit or goat anti-rat IgG (Molecular Probes A-11012, A-11007; Invitrogen). After washing three times in PBS, slides were mounted with Vectashield mounting medium (Vector Laboratories, Burlingame, CA). Images were obtained using a confocal laser-scanning inverted microscope (Olympus IX70 and MRC-1024, BioRad) with an argon–krypton laser. Enhanced green fluorescent protein (EGFP) and Alexa Fluor™ 594 were detected using the 488 nm- and 568 nm-line excitation with 522DF/35 nm and HQ598/40 emission filters, respectively.

Quantification of the number of cells expressing HA-tagged proteins at the membrane surface was calculated as the percentage of red HA-positive fluorescent cells relative to the total cellular pool of green fluorescent cells positively transfected by using GFP as reporter. The non-permeabilized cells were visualized at low magnification (20× objective) by an observer blinded to experimental design, and 100 randomly chosen green-positive cells per coverslip, were scored by eye for the red fluorescence signal. Values represent the mean ± S.D. of cells judged to be positive for surface KCNQ4 staining of three coverslips from four independent transfections.

Results and discussion

Identification of a novel pathogenic mutation (p.G296S) in the pore region of KCNQ4 channel

Based on the current knowledge that affected individuals carrying mutations in *KCNQ4* display high-frequency hearing loss (DFNA2), we designed a phenotype-guided mutational screening in small families which were not suitable for linkage analysis. Thus, probands from 90 unrelated families displaying non-syndromic sensorineural high-frequency hearing loss were then screened for mutations in the *KCNQ4* gene. Forty-three of these probands belonged to families segregating autosomal dominant hearing impairment. In patients of the remaining families the pattern of inheritance could not be defined

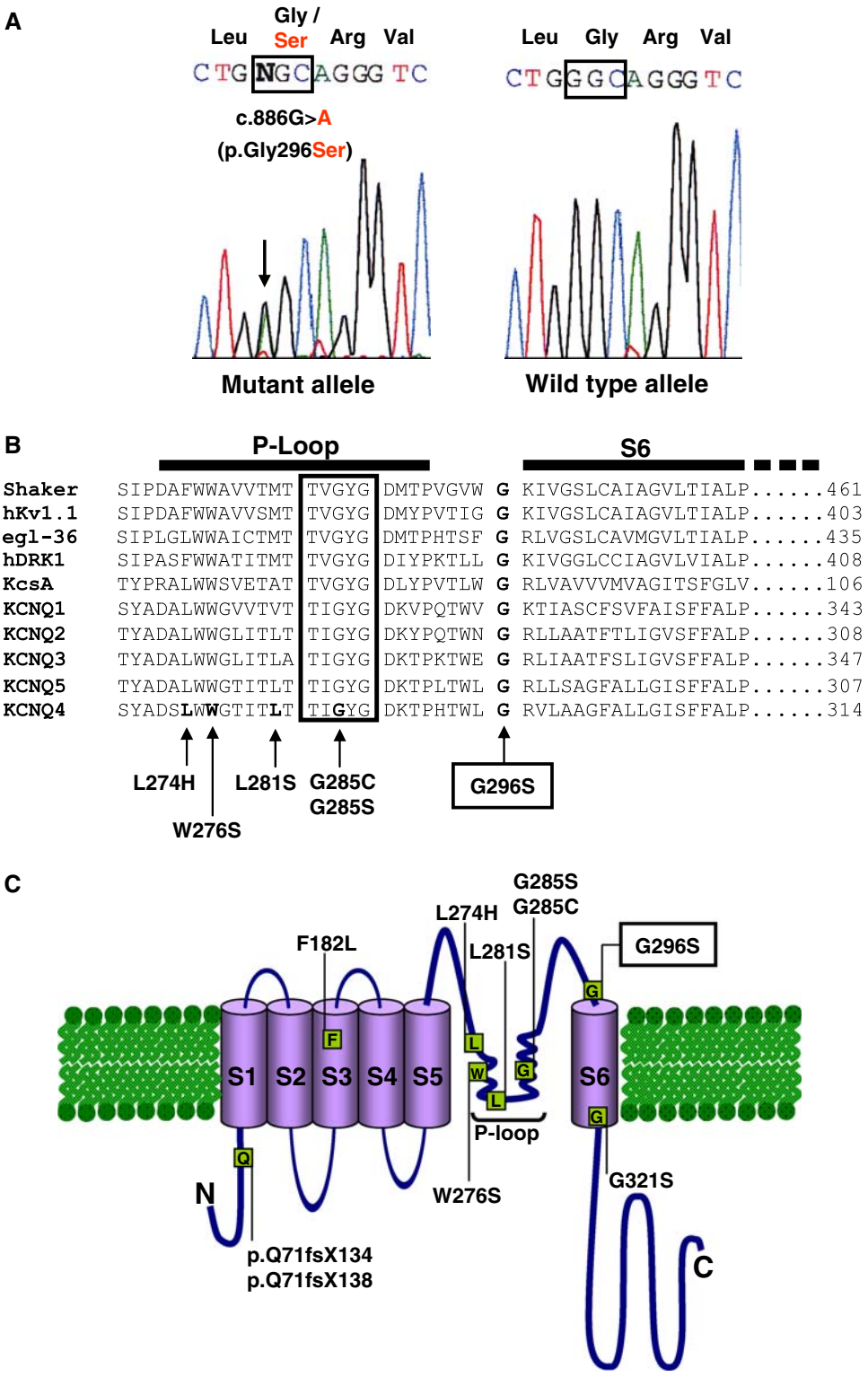

Fig. 2 **a** Electropherogram depicting the *KCNQ4* exon 6 fragment that contains the novel mutation. The *arrow* points to the precise nucleotide that is mutated. **b** Multiple protein alignment of KCNQ4 and homologous proteins in the pore region and partial S6 transmembrane domain. The G296 residue, which is mutated in this family, is indicated in *bold*. The selectivity filter contained in the P-loop domain is *boxed*. All the KCNQ4 pore-region mutations previously described are indicated. The sequences are: Shaker, *Drosophila melanogaster*, (PIR S00479); hKv1.1, *Homo sapiens*, (Swissprot Q09470); egl-36, *Caenorhabditis elegans*, (GenBank AF005246); hDRK1, *Homo sapiens*, (PIR S31761); KcsA, *Streptomyces lividians*, (PIR S60172); KCNQ1–KCNQ5, *Homo sapiens*, (PIR 3953684; 4028015; 2801450; 4262539 and GenBank BC050689). **c** Graphical representation of the KCNQ4 voltage-gated potassium channel (modified from Jentsch 2000). The six transmembrane domains (S1–S6) and the P-loop are indicated. All ten currently known *KCNQ4* mutations are shown (Kubisch et al. 1999; Coucke et al. 1999; Kamada et al 2006; Talebizadeh et al. 1999; Van Hauwe et al. 2000; Akita et al. 2001; Van Camp et al. 2002; Topsakal et al. 2005; Su et al. 2007). The novel mutation, p.G296S, identified in this work is *boxed*

unambiguously. Most of the reported mutations of *KCNQ4* lie in the pore region of the channel, which is encoded by exons 5 and 6. Thus, these exons and flanking intronic regions were PCR amplified from genomic DNA isolated from the ninety probands and the amplified products were analyzed for the presence of heteroduplex. An indication of the presence of a mutation was obtained in exon 6 in the selected proband (III:1) of family S300 (Fig. 1a). Sequencing of the PCR product identified the transition mutation c.886G>A which reveals the p.G296S substitution

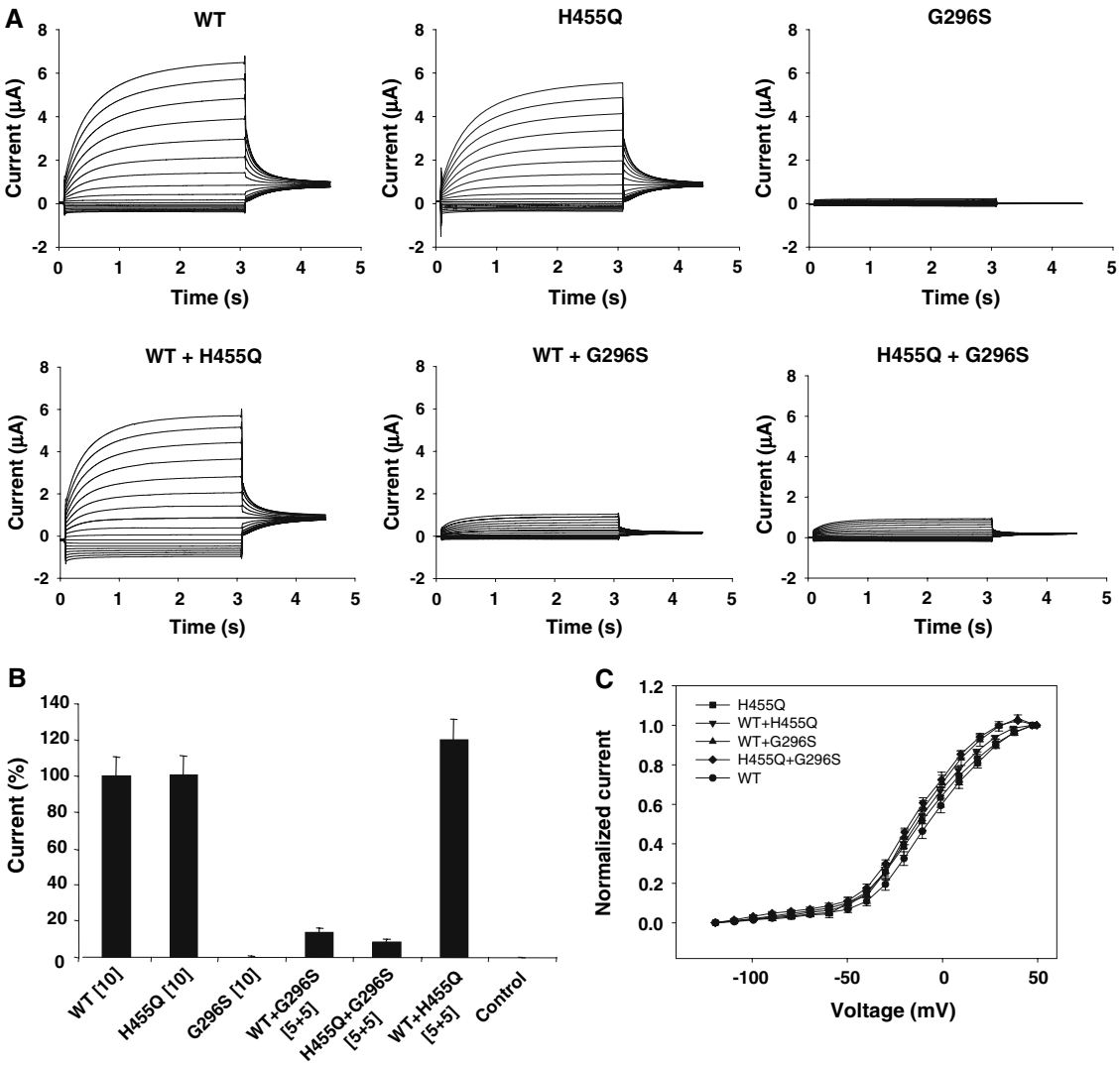

Fig. 3 Functional analysis of the $KCNQ4_{WT}$, $KCNQ4_{H455Q}$ and $KCNQ4_{G296S}$ alleles in *Xenopus* oocytes. Oocytes were independently injected (10 ng/oocyte) or co-injected at 1:1 ratio (5 + 5 ng) with cRNAs of the wild type and mutated KCNQ4 alleles. **a** Sample records of macroscopic currents evoked by voltage pulses of 3 s duration, applied from a holding potential of −50 mV, varying from −120 mV and +50 mV in 10 mV steps, and returning to a constant pulse of −20 mV. Whereas oocytes expressing or co-expressing wild type and $KCNQ4_{H455Q}$ channels exhibited large currents activated upon depolarization, no currents were detected in $KCNQ4_{G296S}$ oocytes. Co-expression of $KCNQ4_{G296S}$ with the wild type or $KCNQ4_{H455Q}$ variant caused a marked reduction in the amplitude of currents. **b** Comparison of the averaged current (%) obtained from several experiments from each group (n = 5 to 16, two oocytes batches, ±SEM). Currents were normalized relative to the maximal averaged value obtained from several experiments in the $KCNQ4_{WT}$ group. Current levels recorded in the $KCNQ4_{G296S}$ oocytes were indistinguishable from those detected in water-injected control oocytes. **c** Comparison of I/V relationships. Curves represent the fitting to a Boltzmann equation of the I/V values obtained for each group of oocytes. There were no significant differences in voltage sensitivity between the wild type ($V_{1/2}$ = -11.86 ± 0.72; Slope = 16.89 ± 0.54) and $KCNQ4_{H455Q}$ channel. Similarly, the co-expression of $KCNQ4_{G296S}$ with the wild type or $KCNQ4_{H455Q}$ variant reduced the magnitude of currents but did not modify the voltage-gating properties. Each point of the different curves represents the I/V mean value (± SE; n = 5 to 16, two oocytes batches) normalized relative to the maximal averaged I/V relationship obtained in each experiment

in the predicted KCNQ4 polypeptide (Fig. 2a). Genotyping of family S300 with microsatellite markers D1S2730, D1S255 and D1S2722 of the DFNA2 region and subsequent linkage analysis yielded LOD scores that corresponded to the simulated maximum value (LOD score = 1.81 at θ = 0) obtained in this family. The mutation was present in the heterozygous state, and generated an additional restriction site for the enzyme *DdeI* at exon 6. We took advantage of this finding to develop a screening test specific for the mutation (see "Patients and methods"). The test showed that the mutation segregated with the hearing-impairment status in the family. In addition, it was not present in 100

unrelated Spanish individuals with normal hearing. The identification of this novel mutation further supports the existence of a cluster of mutations in the pore region of KCNQ4 (Fig. 2c) that is associated in all cases with a characteristic high-frequency hearing loss phenotype. This novel mutation involves a glycine that is placed in the stretch of five amino acids that connects the P-loop domain and the S6 segment. This glycine is perfectly conserved among members of *KCNQ* family as well as of the superfamily of voltage-gating K^+ channels in all species (Fig. 2b). The equivalent glycine is mutated in *KCNQ1* (G325R) in families segregating the autosomal dominant Romano-Ward syndrome, the most common form of long-QT syndrome (Splawski et al. 2000; Donger et al. 1997; Tanaka et al. 1997). To exclude the involvement of other *KCNQ4* mutations in the hearing loss of the family, we sequenced the remaining exons in the affected subjects III:1, IV:2 and IV:5. No other mutation was found apart from the c.1365T>G in the coding region of exon 10 which gives rise to the p.H455Q allelic variant. This allele, in trans with respect to the p.G296S mutation in patient III:1, did not segregate with the hearing loss in the family (Fig. 1a). Indeed, the p.H455Q allele was previously reported as non-pathogenic (Talebizadeh et al. 1999) and it has been further corroborated by the functional studies described below. The DFNA2 locus also contains the connexin 31 encoding gene, *GJB3* (MIM#600101), which has been reported to be responsible for ADNSHL in two Chinese families (Xia et al. 1998). The haplotype analysis for the three microsatellite markers of the DFNA2 region in the S300 family could not exclude the involvement of *GJB3* in the hearing loss, therefore, all exons of this gene were sequenced in individual III:1 (Fig. 1a), but no mutations were found.

Effects of p.G296S mutation on KCNQ4 cell surface expression and channel function

To determine the possible consequences of these two allelic variants, $KCNQ4_{H455Q}$ and $KCNQ4_{G296S}$, on the channel function, KCNQ4 was expressed in *Xenopus* oocytes. $KCNQ4_{WT}$ and $KCNQ4_{H455Q}$ injected oocytes developed hyperpolarization of the resting potential paralleled by an increase in membrane conductance. Quantification of whole cell currents was performed by voltage-clamp analysis. The $KCNQ4_{WT}$ or $KCNQ4_{H455Q}$ expressing oocytes showed outward K^+ currents upon membrane potential depolarization. Typically, activation of K^+ currents was detected around –40 mV, half-maximum activation occurred nearby −11 mV and saturated at +50 mV (Fig. 3c). This voltage dependence corresponds to that described for the KCNQ4 channels in absence of regulatory KCNE-β-subunits (Kubisch et al. 1999; Strutz-Seebohm et al. 2006). Such currents were, however, not recorded in those expressing the $KCNQ4_{G296S}$ mutant and in control water-injected oocytes (Fig. 3a, b). These data clearly indicate that the mutation p.G296S causes a complete loss of channel activity, while the p.H455Q mutation does not affect the functionality of KCNQ4 channels.

The lack of voltage-activated K^+ currents in the $KCNQ4_{G296S}$ injected oocytes might be attributable to a reduction of KCNQ4 channel number in the cell surface or because the mutation impairs the channel function. Total expression of KCNQ4 protein and its relative cell-surface abundance was determined by Western blot analysis (Fig. 4a, b). The total amount of KCNQ4 channel protein (cytoplasmic plus surface located) produced by the oocytes was estimated from the whole cell lysates. For wild type and mutant oocytes injected with the same amount of cRNA (5 ng/oocyte), KCNQ4 antibody detected a monomer band of similar intensity with an apparent molecular weight of ~65 kDa (Kharkovets et al. 2000), indicating that there are no differences in protein synthesis and turnover. Cell-surface expression was estimated by biotinylation of membrane KCNQ4 protein with the membrane-

Fig. 4 The G296S mutant impairs in a dominant manner the cell-surface expression of wild type KCNQ4 channels. **a**, **b** Oocytes were injected with water (control), $KCNQ4_{WT}$ and mutant $KCNQ4_{G296S}$ cRNA alone (5 ng/oocyte) or with a 1:1 mixture of wild type and mutant RNAs (WT+G296S) at low and high concentration (5 and 10 ng/oocyte). After 72 h, electrophysiological recordings were performed in oocytes before being collected for Western blotting. **a** Representative Western blots of total and biotinylated surface KCNQ4 protein detected with an anti-KCNQ4 antibody directed against carboxy-terminal peptides. **b** Band intensities from total and surface blots quantified by densitometry (*black bars*; mean ± SE from $n = 4$ experiments, 35 oocytes per reaction). Mean current at the end of +50 mV pulses and 2 s duration recorded in the same batches of oocytes used for Western blotting (*white bars* in bottom panel). Values of band intensity and current amplitude were normalized, for each experiment, to those obtained for $KCNQ4_{WT}$ cRNA injected oocytes (5 ng/oocyte). For equal total expression of $KCNQ4_{WT}$ and mutant $KCNQ4_{G296S}$ protein, cell-surface abundance of the mutant was strongly reduced ($^*P < 0.05$; paired t test) and records did not show K^+ currents over background level of control oocytes ($^{**}P > 0.05$; paired t test). In experiments of co-expression (WT+G296S), the mutant reduced cell-surface KCNQ4 expression and K^+ currents in the same amount. **c**, **d** Oocytes were injected with 5 and 0.5 ng of $KCNQ4_{WT}$ or 10 ng of mutant $KCNQ4_{G296S}$ cRNAs, and with water in control. **c** Total and surface KCNQ4 expression normalized to the values of wild type oocytes injected with 5 ng (mean ± SE; $n = 3$). **d** Sample currents (I_m) recorded in control, $KCNQ4_{WT}$ and mutant $KCNQ4_{G296S}$ injected oocytes using a typical voltage protocol for KCNQ4 channel activation (V_m). Note that the $KCNQ4_{WT}$ oocytes injected with 0.5 ng of cRNA that showed a faint band of surface KCNQ4 expression still exhibited voltage-activated K^+ currents. In contrast, the currents recorded in $KCNQ4_{G296S}$ oocytes injected with 10 ng of cRNA, that yielded a higher expression of KCNQ4 at membrane surface, were indistinguishable from those obtained in controls, indicating that this mutation causes, in addition to the defect in trafficking, a complete loss of channel function

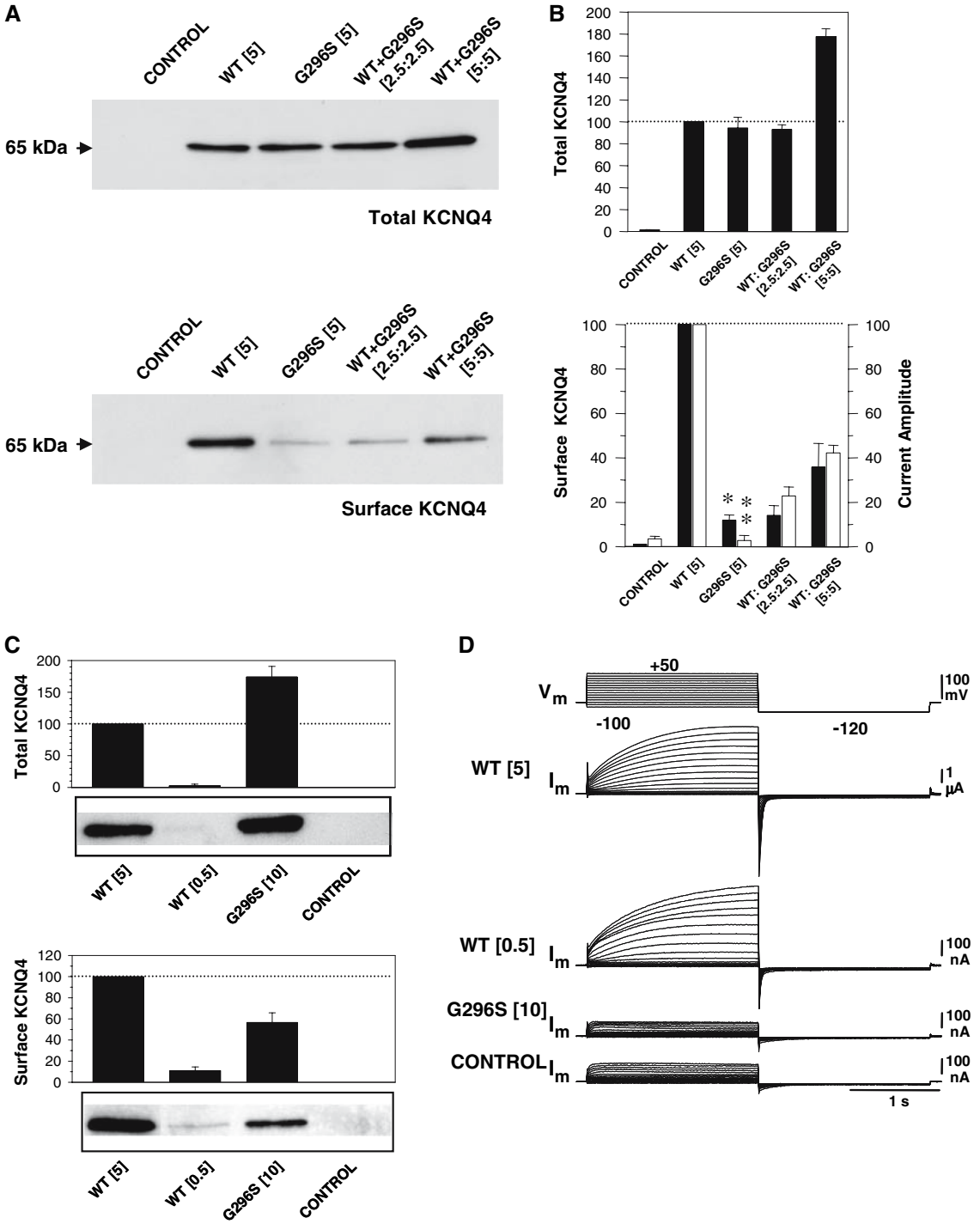

impermeable *N*-hydroxysuccinimide-SS-biotin reagent. While a robust band of $KCNQ4_{WT}$ was detected, the abundance of $KCNQ4_{G296S}$ mutant protein at the cell surface was reduced by 88.03±2.31%, indicating that the mutation altered profoundly the steady state distribution of KCNQ4 channels due to cytoplasmic retention of mutant protein. A defect in trafficking/surface expression can be determined by the alteration of diverse mechanisms, including folding, assembly, endoplasmic reticulum (ER) retention/retrieval or ER export signals (Ellgaard and Helenius 2003). The minor fraction of mutant KCNQ4 channels that was still able to reach the plasma membrane did not yield voltage-activated K^+ currents, indicative of that the pore-region mutation impairs the channel functionality, presumably because its location within the pore region. For wild type-injected oocytes, the voltage-activated K^+

currents were still detected over background level of water-injected oocytes when the amount of RNA injected was reduced from 5 to 0.5 ng/oocyte (Fig. 4c, d). With this RNA concentration the level of KCNQ4 expression at cell surface was approximately similar to that observed for the mutant oocytes injected with 5 ng (Fig. 4a, b). When the mutant expression at the cell surface was forced by increasing amount of RNA injected (10 ng/oocyte), which yielded higher levels than in the wild type injected with 0.5 ng, records did not show any current attributable to the voltage activation of KCNQ4 channels (Fig. 4c, d). Taken together, these results seem to confirm that the p.G296S mutation also causes a loss of channel function.

The deficient surface expression of mutant $KCNQ4_{G296S}$ was further corroborated by immunochemistry in NIH-3T3 cells transiently transfected with the KCNQ4 tagged extracellularly with HA epitope (see "Patients and methods"). As shown in Fig. 5a, b, the red staining (HA-positive) in non-permeabilized cells was detected in the membrane surface of a vast majority of GFP-positive cells transfected with the $KCNQ4_{WT}$ (97 ± 2.3%), but not in the GFP-positive cells transfected with the $KCNQ4_{G296S}$ variant (3 ± 1.5%). For comparative purposes, we used the affinity-purified antisera raised against KCNQ4 intracellular peptides (anti-KCNQ4). As expected, this staining pattern at the cell surface was not appreciated in the non-permeabilized cells when using anti-KCNQ4 (Fig. 5c). Immunostaining of wild type and mutant KCNQ4 protein located intracellularly was observed in permeabilized cells when using either anti-HA and anti-KCNQ4 antibodies (Fig. 5b, c). Collectively, these data are consistent with the biotinylation assays and reveal a differential processing to surface expression of mutant channels in comparison with wild type KCNQ4 channels.

Effect of G296S mutant on the trafficking of wild type KCNQ4 channels

To mimic the heterozygous condition observed in the patients, oocytes were co-injected with a 1:1 mixture of mutant alleles and wild type KCNQ4 cRNAs (Fig. 3a–c). Upon co-expression of $KCNQ4_{H455Q}$ with $KCNQ4_{WT}$, the amplitude of K^+ currents was similar to those generated for the same final RNA concentration of each one alone. In contrast, when the $KCNQ4_{G296S}$ mutant was co-injected with $KCNQ4_{WT}$ or $KCNQ4_{H455Q}$, the amplitude of currents reduced by 90 ± 2.4%. This reduction in K^+ currents was not associated with changes in the kinetic properties and voltage sensitivity or with a shift in the reversal potential of tail currents (Fig. 3c). The magnitude of dominant-negative effect that the G296S mutant exerts on wild-type KCNQ4 activity is similar to that previously reported for another DFNA2 mutation, the p.G285S substitution (Kubisch et al. 1999).

To determine the mechanism by which the G296S mutant exerts this potent dominant-negative effect on wild type KCNQ4 currents, we performed co-expression studies in which oocytes were injected with a 1:1 mixture of wild type and mutant KCNQ4 cRNA at two final concentrations, low (5 ng/oocyte) and high (10 ng/oocyte). Total protein expression induced by co-injections with the low and high cRNA concentrations were respectively equal and double to that obtained for the oocytes injected with the wild type or mutant cRNA alone (5 ng/oocyte), reflecting linearity in the expression of both proteins with the amount of cRNA injected (Fig. 4a, b, upper panels). However, co-injections with the G296S mutant resulted in potent decreases in cell surface expression of KCNQ4, and in a parallel reduction in the amplitude of K^+ currents (Fig. 4a, b, bottom panels). For low and high (cRNA) co-injections, the surface expression decreased respectively to the 14.11 ± 4.37 and 35.76 ± 15.71% relative to wild type (5 ng/oocyte). The normalization for the difference in total KCNQ4 expression showed a similar reduction in surface expression for the two RNA concentrations (Fig. 4b, bottom), indicating that the effect of dominant inhibition depends on the ratio of wild type and mutant subunits rather than on the absolute amount of mutant protein expressed. Thus, the mutant could suppress KCNQ4 channels at the cell surface through heteromerization with wild type subunits rather than by interfering with the folding or assembly. Our biochemical and electrophysiological data are consistent with the hypothesis that the incorporation of mutant subunits in the tetrameric complexes decreases the efficiency of channels to be exported to cell surface and hence, it reduces the amplitude of KCNQ4 currents. The percentage of reduction in cell-surface expression and channel activity caused by the mutant when it was co-expressed with wild type at 1:1 ratio (i.e., the heterozygous state of patients) is somewhat smaller than the theoretically expected for a "pure" dominant negative effect with only the WT homotetramers (1/16) being exported and functional (MacKinnon 1991). Thus, it is likely that a part of K^+ currents may be accounted by heterotetramers with electrophysiological properties similar to those of the WT channels.

The ER export of potassium channels like other membrane proteins is limited by folding and assembly and may be under the control of specific export signals that reside on component subunits (Ma and Jan 2002). Our results of the pore channel mutation p.G296S may indicate that the structural integrity of the channel-pore domain is a requirement for the efficient surface expression of KCNQ4 channel. In keeping with this proposal, a critical determinant in controlling surface expression of *Shaker*-related or Kv1 subfamily of voltage-gated K^+ channels has been

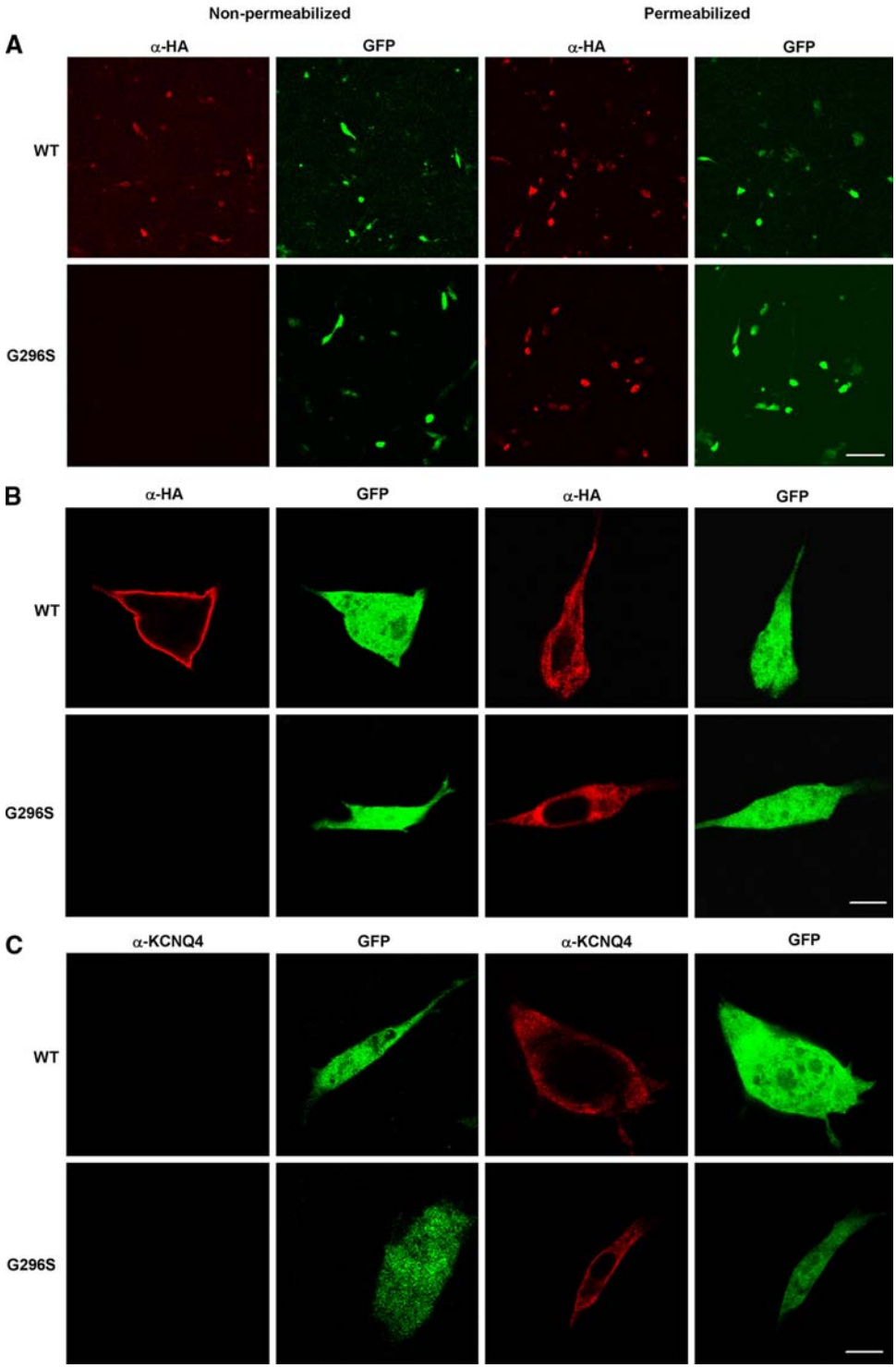

Fig. 5 Defective cell-surface expression of the HA-tagged mutant $KCNQ4_{G296S}$ in NIH-3T3 transfected cells. The HA epitope was inserted in the extracellular loop between the S1 and S2 transmembrane domains. GFP expression was used as reporter of the positive-transfected cells (*in green*). **a**, **b** Confocal images at low- and high-magnification (*upper and bottom panels*) showing that the staining at the cell surface of $KCNQ4_{WT}$ with α-HA antibody (*in red*) in non-permeabilized (*left column*) was absent in cells transfected with the mutant $KCNQ4_{G296S}$. The expression of the wild type and mutant KCNQ4 proteins was confirmed in permeabilized cells (*right column*). **c** Cytoplasmic staining with a α-KCNQ4 antibody raised against carboxy-terminal peptides was performed for comparative purposes. Unlike in permeabilized cells, no staining was observed in non-permeabilized cells transfected with the wild type and mutant HA-tagged KCNQ4 proteins, *Scale bars*, 100 μm in **a**; 10 μm in **b** and **c**

located to the highly conserved potassium channel pore (Manganas et al. 2001). However, these data do not exclude the possibility that the cytoplasmic C terminus can further influence KCNQ channel assembly and surface expression (Schwake et al. 2003, 2006; Kanki et al. 2004; Howard et al. 2007). Indeed, in another KCNQ channel, KCNQ1, several mutations within the C-terminal domain associated with long-QT syndrome type 1 reduce significantly the number of functional channels on the cell surface in a dominant negative fashion (Kanki et al. 2004). Also, there are KCNQ1 mutations in the pore region that disrupt the transport to the cell surface of potassium channels causing a dominant-negative effect (Shalaby et al. 1997; Wollnik et al. 1997). In this context, it would be interesting

to determine whether the defect in channel trafficking is a specific effect of the p.G296S mutation or is one common mechanism for the other missense DFNA2 mutations clustered in the pore region of KCNQ4 channel in which the effect of dominant-inhibition has already been reported (Kubisch et al. 1999; Jentsch 2000).

Pathogenesis of DFNA2 hearing loss

The pathogenic mechanisms that lead to a progressive high-frequency DFNA2 hearing loss have been a matter of debate during the last years. Degeneration of both types of cochlear sensory cells (Kubisch et al. 1999; Oliver et al. 2003; Beisel et al. 2000, 2005) or a central auditory pathway defect (Kharkovets et al. 2000) emerged as reasonable explanations for this pathology. Our clinical data (see "Patients and methods") of abnormal transient-evoked otoacoustic emissions (TEOAEs), which measures the activity of the OHCs, but preserved auditory brainstem responses (ABRs) in terms of wave latency and interlatency observed in the young patients IV:5 (9 years) and IV:1 (17 years) confirm a defect of the OHCs and exclude the involvement of the central auditory pathway, at least in the early stage of DFNA2 pathology. The mouse model appears to recapitulate the hearing loss observed in the patients with missense mutations. Transgenic mice in which the *Kcnq4* gene carried in heterozygous state the dominant-negative mutation p.G285S in the pore-region developed a slow progressive hearing loss that was paralleled by a selective degeneration of OHCs of the basal (high frequency) turns (Kharkovets et al. 2006). The electrophysiological studies in these OHCs show a reduction in the overall KCNQ4 currents, and a chronic depolarization of resting membrane potential preceding to degenerative changes. Because the p.G296S mutant exerts a dominant-negative effect on the KCNQ4 channel activity similar to that observed for the p.G285S mutation, it is tempting to speculate that both mutations can share a common mechanism of pathogenesis. Our results show for the first time that the loss of ionic currents results from a defect in trafficking of KCNQ4 channels to the cell membrane. If this mechanism is confirmed for the other KCNQ4 dominant-negative mutations, some emerging strategies to correct protein trafficking abnormalities would be applicable to DFNA2 pathology (Rowe et al. 2005; Anderson et al. 2006).

Acknowledgments We thank members of the Spanish family, whose participation made this study possible. We also express our gratitude to T.J. Jentsch for kindly providing antibodies and to A. Muñoz, PhD, for technical assistance. This work was supported by grants from the Spanish Ministerio de Ciencia y Tecnología (SAF 2002-03966; BFI 2003-00693; SAF 2005-03414 to L.C.B.), Spanish Fondo de Investigaciones Sanitarias (FIS G03/203; CP03/00014), Programa Ramón y Cajal (to I.d.C); Fundación Ramón Areces and European Union (FP6 Integrated Project EUROHEAR, LSHG-CT-2004-512063; SLMM-CT-2004-50303) and from the Comunidad Autónoma de Madrid (Programa de Biociencias en Ingeniería Biomédica MADR.IB, S2006/SAL-0312 to L.C.B).

References

Akita J, Abe S, Shinkawa H, Kimberling WJ, Usami S (2001) Clinical and genetic features of nonsyndromic autosomal dominant sensorineural hearing loss: KCNQ4 is a gene responsible in Japanese. J Hum Genet 46:355–361

Anderson CL, Delisle BP, Anson BD, Kilby JA, Will ML, Tester DJ, Gong Q, Zhou Z, Ackerman MJ, January CT (2006) Most LQT2 mutations reduce Kv11.1 (hERG) current by a class 2 (trafficking-deficient) mechanism. Circulation 113:365–373

Balatsouras D, Kaberos A, Karapantzos E, Homsioglou E, Economou NC, Korres S (2004) Correlation of transiently evoked otoacoustic emission measures to auditory thresholds. Med Sci Monit 10:MT24–30

Beisel KW, Nelson NC, Delimont DC, Fritzsch B (2000) Longitudinal gradients of KCNQ4 expression in spiral ganglion and cochlear hair cells correlate with progressive hearing loss in DFNA2. Mol Brain Res 82:137–149

Beisel KW, Rocha-Sánchez S, Morris KA, Nie L, Feng F, Kachar B, Yamoah EN, Fritzsch B (2005) Differential expression of KCNQ4 in inner hair cells and sensory neurons is the basis of progressive high-frequency hearing loss. J Neurosci 25:9285–9293

Coucke P, Van Camp G, Djoyodiharjo B, Smith SD, Frants RR, Padberg GW, Darby JK, Huizing EH, Cremers CW, Kimberling WJ, Oostra BA, Van de Heyning PH, Willems PJ (1994) Linkage of autosomal dominant hearing loss to the short arm of chromosome 1 in two families. N Engl J Med 331:425–431

Coucke PJ, Van Hauwe P, Kelley PM, Kunst H, Schatteman I, Van Velzen D, Meyers J, Ensink RJ, Verstreken M, Declau F, Marres H, Kastury K, Bhasin S, McGuirt WT, Smith RJH, Cremers CWRJ, Van de Heyning P, Willems PJ, Smith SD, Van Camp G (1999) Mutations in the KCNQ4 gene are responsible for autosomal dominant deafness in four DFNA2 families. Hum Mol Genet 8:1321–1328

Dib C, Faure S, Fizames C, Samson D, Drouot N, Vignal A, Millasseau P, Marc S, Hazan J, Seboun E, Lathrop M, Gyapay G, Morissette J, Weissenbach J (1996) A comprehensive genetic map of the human genome based on 5,264 microsatellites. Nature 380:152–154

Donger C, Denjoy I, Berthet M, Neyroud N, Cruaud C, Bennaceur M, Chivoret G, Schwartz K, Coumel P, Guicheney P (1997) KVLQT1 C-terminal missense mutation causes a forme fruste long-QT syndrome. Circulation 96:2778–2781

Doyle DA, Morais-Cabral J, Pfuetzner RA, KuoA, Gulbis JM, Cohen SL, Chait BT, MacKinnon R (1998) The structure of the potassium channel: molecular basis of K+ conduction and selectivity. Science 280:69–77

Ellgaard L, Helenius A (2003) Quality control in the endoplasmic reticulum. Nat Rev Mol Cell Biol 4: 181–191

Etxeberria A, Santana-Castro I, Regalado MP, Aivar P, Villarroel A (2004) Three mechanisms underlie KCNQ2/3 heteromeric potassium M-channel potentiation. J Neurosci 24:9146–9152

Friedman TB, Griffith AJ (2003) Human nonsyndromic sensorineural deafness. Annu Rev Genom Hum Genet 4:341–412

Howard RJ, Clark KA, Holton JM, Minor DL Jr (2007) Structural insight into KCNQ (Kv7) channel assembly and channelopathy. Neuron 53:663–675

Jentsch TJ (2000) Neuronal KCNQ potassium channels: physiology and role in disease. Nat Rev 1:21–30

Kamada F, Kure S, Kudo T, Suzuki Y, Oshima T, Ichinohe A, Kojima K, Niihori T, Kanno J, Narumi Y, Narisawa A, Kato K, Auki Y, Ikeda K, Kobayashi T, Matsubara Y (2006) A novel KCNQ4 one-base deletion in a large pedigree with hearing loss: implication for the genotype-phenotype correlation. J Hum Genet 51:455–460

Kanki H, Kupershmidt S, Yang T, Wells S, Roden DM (2004) A structural requirement for processing the cardiac K^+ channel KCNQ1. J Biol Chem 279:33976–33983

Kharkovets T, Hardelin JP, Safieddine S, Schweizer M, El-Amraoui A, Petit C., Jentsch TJ (2000) KCNQ4, a K+ channel mutated in a form of dominant deafness, is expressed in the inner ear and the central auditory pathway. Proc Natl Acad Sci USA 97:4333–4338

Kharkovets T, Dedek K, Maier H, Schweizer M, Khimich D, Nouvian R, Vardanyan V, Leuwer R, Moser T, Jentsch TJ (2006) Mice with altered KCNQ4 K+ channels implicate sensory outer hair cells in human progressive deafness. EMBO J 25:642–652

Kubisch C, Schroeder BC, Friedrich T, Lutjohann B, El-Amraoui A, Marlin S, Petit C, Jentsch TJ (1999) KCNQ4, a novel potassium channel expressed in sensory outer hair cells, is mutated in dominant deafness. Cell 96:437–446

Lorenz C, Pusch M, Jentsch TJ (1996) Heteromultimeric CLC chloride channels with novel properties. Proc Natl Acad Sci USA 93:13362–13366

Ma D, Jan LY (2002) ER transport signals and trafficking of potassium channels and receptors. Curr Opin Neurobiol 12:287–292

MacKinnon R (1991) Determination of the subunits stoichiometry of a voltage-activated potassium channel. Nature 350:232–235

Manganas LN, Wang Q, Scannevin RH, Antonucci DE, Rhodes KJ, Trimmer JS (2001) Identification of a trafficking determinant localized to the Kv1 potassium channel pore. Proc Natl Acad USA 98:14055–14059

Oliver D, Knipper M, Derst C, Fakler B (2003) Resting potential and submembrane calcium concentration of inner hair cells in the isolated mouse cochlea are set by KCNQ-type potassium channels. J Neurosci 23:2141–2149

Petersen MB (2002) Non-syndromic autosomal-dominant deafness. Clin Genet 62:1–13

Petersen MB, Willems PJ (2006) Non-syndromic, autosomal-recessive deafness. Clin Genet 69:371–392

Rowe SM, Miller S, Sorscher EJ (2005) Cystic fibrosis. N Engl J Med 352:1992–2001

Schwake M, Pusch M, Kharkovets T, Jentsch TJ (2000) Surface expression and single channel properties of KCNQ2/KCNQ3, M-type K^+ channels involved in epilepsy. J Biol Chem 18:13343–13348

Schwake M, Jentsch TJ, Friedrich T (2003) A carboxy-terminal domain determines the subunit specificity of KCNQ K^+ channel assembly. EMBO Rep 4:76–81

Schwake M, Athanasiadu D, Beimgraben C, Blanz J, Beck C, Jentsch TJ, Saftig P, Friedrich T (2006) Structural determinants of M-type KCNQ (K_v7) K^+ channel assembly. J Neurosci 26:3757–3766

Shalaby FY, Levesque PC, Yang WP, Little WA, Conder ML, Jenkins-West T, Blanar MA (1997) Dominant-negative KvLQT1 mutations underlie the LQT1 form of long QT syndrome. Circulation 96:1733–1736

Splawski I, Shen J, Timothy KW, Lehmann MH, Priori S, Robinson JL, Moss AJ, Schwartz PJ, Towbin JA, Vincent GM, Keating MT (2000) Spectrum of mutations in long-QT syndrome genes. KVLQT1, HERG, SCN5A, KCNE1, and KCNE2. Circulation 102:1178–1185

Strutz-Seebohm M, Seebohm G, Fedorenko O, Baltaev R, Engel J, Knirsch M, Lang F (2006) Functional co-assembly of KCNQ4 with KCNE-β-subunits in *Xenopus* oocytes. Cell Physiol Biochem 18:57–66

Su CC, Yang JJ, Shieh JC, Su MC, Li SY (2007) Identification of novel mutations in the KCNQ4 gene of patients with nonsyndromic deafness from Taiwan. Audiol Neurootol 12:20–26

Talebizadeh Z, Kelley PM, Askew JW, Beisel KW, Smith SD (1999) Novel mutation in the KCNQ4 gene in a large kindred with dominant progressive hearing loss. Hum Mutat 14:493–501

Tanaka T, Nagai R, Tomoike H, Takata S, Yano K, Yabuta K, Haneda N, Nakano O, Shibata A, Sawayama T, Kasai H, Yazaki Y, Nakamura Y (1997) Four novel KVLQT1 and four novel HERG mutations in familial long-QT syndrome. Circulation 95:565–567

Topsakal V, Pennings RJ, te Brinke H, Hamel B, Huygen PL, Kremer H, Cremers CW (2005) Phenotype determination guides swift genotyping of a DFNA2/KCNQ4 family with a hot spot mutation (W276S). Otol Neurotol 26:52–58

Van Camp G, Coucke PJ, Kunst H, Schatteman I, Van Velzen D, Marres H, Van Ewijk M, Declau F, Van Hauwe P, Meyers J, Kenyon J, Smith SD, Smith RJH, Djelantik B, Cremers CWRJ, Van de Heyning PH, Willems PJ (1997) Linkage analysis of progressive hearing loss in five extended families maps the DFNA2 gene to a 1.25-Mb region on chromosome 1p. Genomics 41:70–74

Van Camp G, Coucke PJ, Akita J, Fransen E, Abe S, De Leenheer EM, Huygen PL, Cremers CW, Usami S (2002) A mutational hot spot in the KCNQ4 gene responsible for autosomal dominant hearing impairment. Hum Mutat 20:15–19

Van Hauwe P, Coucke PJ, Ensink RJ, Huygen P, Cremers CW, Van Camp G (2000) Mutations in the KCNQ4 K+ channel gene, responsible for autosomal dominant hearing loss, cluster in the channel pore region. Am J Med Genet 93:184–187

Wollnik B, Schroeder BC, Kubish C, Esperer HD, Wieacker P, Jentsch TJ (1997) Pathophysiological mechanisms of dominant and recessive KvLQT1 K^+ channel mutations found in inherited cardiac arrhythmias. Hum Mol Genet 6:1943–1949

Xia JH, Liu CY, Tang BS, Pan Q, Huang L, Dai HP, Zhang BR, Xie W, Hu DX, Zheng D, Shi X, Wang D, Xia K, Yu K, Liao X, Fena Y, Yang Y, Xiao J, Xie D, Huang J (1998) Mutations in the gene encoding gap junction protein beta-3 associated with autosomal dominant hearing impairment. Nat Genet 20:370–373